



New approach to predict load-displacement curves of bored piles in homogeneous sandy soils: numerical analyses

Naloan C. Sampa¹, Tamara B. Correa¹, Pablo G. Oliveira¹

¹*Dept. of Civil Engineering, Federal University of Santa Catarina*

João Pio Duarte da Silva - 205, 88040-900, Santa Catarina, Brazil

naloan.sampa@ufsc.br, tamara.bitten@gmail.com, pablo.gondim.oliveira@gmail.com

Abstract. Large-diameter bored piles are increasingly used in the foundations of bridges, viaducts, and high-rise buildings. This paper proposes a normalized equation to predict the load-displacement curve of bored piles in homogeneous sandy soils from the results of numerical analyses. Geotechnical investigation data and load test results from Araquari Experimental Field were used to calibrate the numerical model run in Abaqus. Appropriate simplifications were made to facilitate the analysis without compromising the representativeness of the real conditions. Sixteen numerical analyses were performed in Abaqus, simulating load tests on piles of four different diameters and four different lengths. The Mohr-Coulomb plasticity criterion was used to model the granular behavior of the soil, while a linear elastic model represented the behavior of the pile due to its stiffness compared to the soil. Based on the results of the numerical analysis, the total loads obtained by the model were compared with those estimated by semi-empirical methods and measured in the in-situ load tests. A normalized equation has been proposed to estimate the load-displacement curves. It is concluded that the methodology adopted in this work was appropriate and the analysis results were satisfactory, contributing to the understanding of the behavior of bored piles.

Keywords: load transfer, normalization, pile interaction mechanism, Abaqus, Araquari Experimental Field.

1 Introduction

Deep foundations utilizing piles are extensively employed to resist and transfer superstructure loads to the soil. The load transfer mechanism involves both lateral friction and pile tip resistance, contingent upon the characteristics of the pile, soil, and applied load. Load testing is a prevalent method for predicting pile behavior, yielding load-displacement curves. Numerous studies (Fleming, [1]; Liu et al. [2]; and others) have developed methods to predict these curves using hyperbolic functions, which consider parameters related to the initial stiffness and asymptote of the curve, calibrated manually based on soil parameters and pile characteristics.

This study aims to introduce a rational formula for predicting the load-displacement curve of individual bored piles in homogeneous sandy soils, derived from numerical modeling results. Additionally, the bearing capacity of bored piles obtained from the numerical model was compared with estimates from semi-empirical methods proposed by Aoki-Velloso [3], Décourt-Quaresma [4], and Teixeira [5], which are widely utilized in Brazil.

2 Material and Methods

Sixteen static load tests were numerically simulated to investigate the effect of varying pile diameter and length on load mobilization and interaction mechanisms. The reference diameter (D_{ref}) and reference length (L_{ref}) were established as 1 m and 24.25 m, respectively, based on the dimensions of the tested piles in Araquari Experimental Field (AEF). The embedded pile lengths were 6.21 m, 12.28 m, 18.34 m, and 24.25 m, considering a free length of 0.15 m above the ground. The diameters were 0.25 m, 0.50 m, 1.00 m, and 1.50 m.

The field tests conducted in AEF (area of 0.3 km²) in Santa Catarina, Brazil, revealed seven distinct layers predominantly composed of compact to loose sands, with a relative density ranging from 27% to 75%. An intermediate layer of silty-sandy clay is found at depths of 18 m to 22 m. The moisture content ranges from 10%

to 70%, N_{SPT} from 5 to 30, the corrected cone tip resistance (q_t) from 2.5 MPa and 10 MPa, the peak friction angle ranges from 23.3° to 38°, the critical friction angle from 22.8° and 35.9°, and the void ratio from 0.61 and 0.95 (Lavalle [6]). The groundwater table was observed to be approximately 3 m below the ground surface (Nienov, [7]). Further details about the experimental field and load tests are available in Nienov's work [7].

A simplified single-layer model was adopted for two key reasons: (1) the challenges associated with calibrating seven-layer numerical models simultaneously (as discussed by Costa [8], and Sampa, Costa, and Nienov [9]), and (2) the difficulty of deriving a rational equation given the numerous variables involved. It is important to clarify that the primary objective of this paper is not to directly compare the results with AEF load tests, as several simplifications were made. Instead, the focus is on developing a rational equation to predict the load-displacement behavior of bored piles in homogeneous soils. The mean geotechnical parameters (Tab. 1) have been determined through a weighted average of the values observed across the seven layers, using Eq. 1.

$$x = \left(\sum_{i=1}^n x_i \cdot h_i \right) / \left(\sum_{i=1}^n h_i \right) \quad (1)$$

where x is the weighted value of the parameter, x_i is the value of the parameter for layer i , and h_i is the thickness of layer i .

Parameter	Value	Parameter	Value
Peak internal frictional angle - ϕ_p (°)	33.091	Permeability coefficient - k (m/s)	0.0001
Dilatancy angle - ψ (°)	1.134	Initial void ratio - e_0	0.759
Lateral earth pressure at rest - K_0	0.454	Cohesion - c (kN/m ²)	7.965
Elastic Module - E (GPa)	33.402	Bulk unit weight - γ (kN/m ³)	18.870
Poisson's ratio - ν	0.3	Friction coefficient - μ	0.627

Table 1. Geotechnical parameters of the granular material.

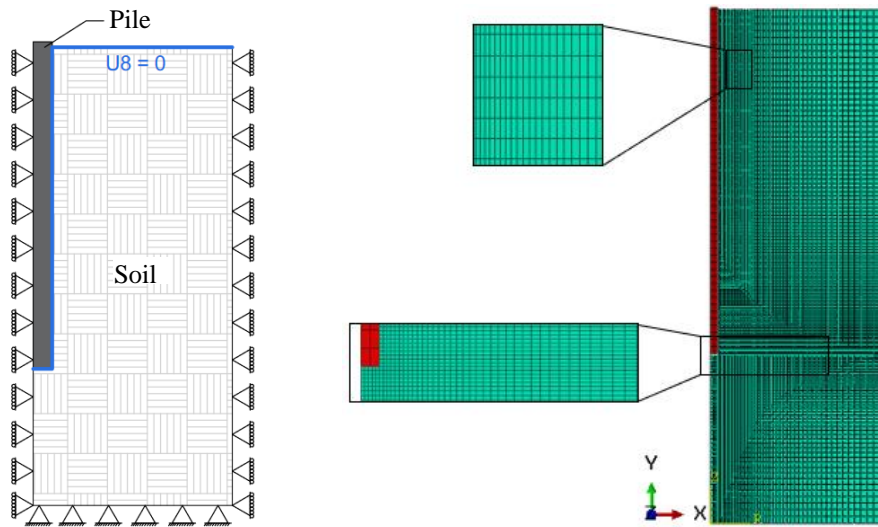


Figure 1. Boundary conditions and mesh of the discretized model.

Vertical load tests were simulated through two-dimensional Finite Element (FE) model, using Abaqus software. To account for the symmetry, it was modeled a half-soil domain with dimensions of 12.5 m in length (12.5 times pile diameter), and 36.25 m in depth (1.5 times the reference pile length). The domain size was deliberately enlarged to minimize significant boundary effects on computed displacement, deformation, and stress. Refined meshing was applied around the pile tip (Fig. 1).

Both vertical and horizontal displacements were constrained at the base, while only horizontal displacement was restricted on the right side and along the symmetry axis. To simulate groundwater and saturated soil conditions, a pore pressure of 0 kPa was imposed on the ground surface.

The pile was modeled as elastic, with a Young's modulus of 40.33 GPa and a Poisson's ratio of 0.3. The soil was defined as an elastoplastic material following the Mohr-Coulomb failure criterion. Saturated soil layers used solid homogeneous elements with pore pressure (CAX4RP), while the pile used CAX4R elements.

Pile-soil interactions were modeled using a surface-to-surface contact approach with a master-slave algorithm. Contacts were treated as hard and normal to interfaces, with shear contact between soil and pile simulated through the Coulomb friction model. The friction coefficient was related to the critical friction angle ($\mu = \tan \phi_{cv}$).

The vertical load test simulation consisted of three steps: geostatic analysis, pile installation, and the load test. The initial step established the self-weight stress field using a body force option and a K_0 derived from $1 - \sin \phi$. The deactivation technique was employed during pile installation, as accurately replicating the in-situ stress conditions during numerical simulation is extremely complex. In the third step, a displacement boundary condition was applied, allowing a maximum displacement of 10% of the D_{ref} (0.1 m), aligned with experimental load tests conducted at the AEF.

The soil parameters from Tab. 1 and the reference pile dimensions were used to calibrate the numerical model. A closer match between the experimental and numerical curves (Fig. 2) was obtained by adjusting the coefficient of earth pressure at rest (K_0) from 0.454 to 0.51. After calibration, 16 numerical simulations were performed, varying pile dimensions while keeping soil and pile properties constant.

The numerical results were used to develop a normalized expression for estimating the load-displacement curve and were compared with estimates from semi-empirical methods.

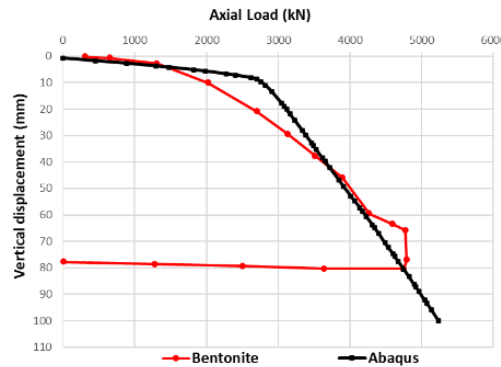


Figure 2. Comparison between experimental and numerical load – displacement curves.

3 Results and Discussion

The load-displacement curves (Fig. 3) indicate that total loads (Q_t) increase with pile length and displacement for piles of the same diameter. In addition, total loads increase with pile diameter for piles of the same length. This observation is consistent with expectations, as piles with larger diameters and lengths provide greater tip and lateral surface areas, respectively, resulting in increased tip resistance and lateral friction.

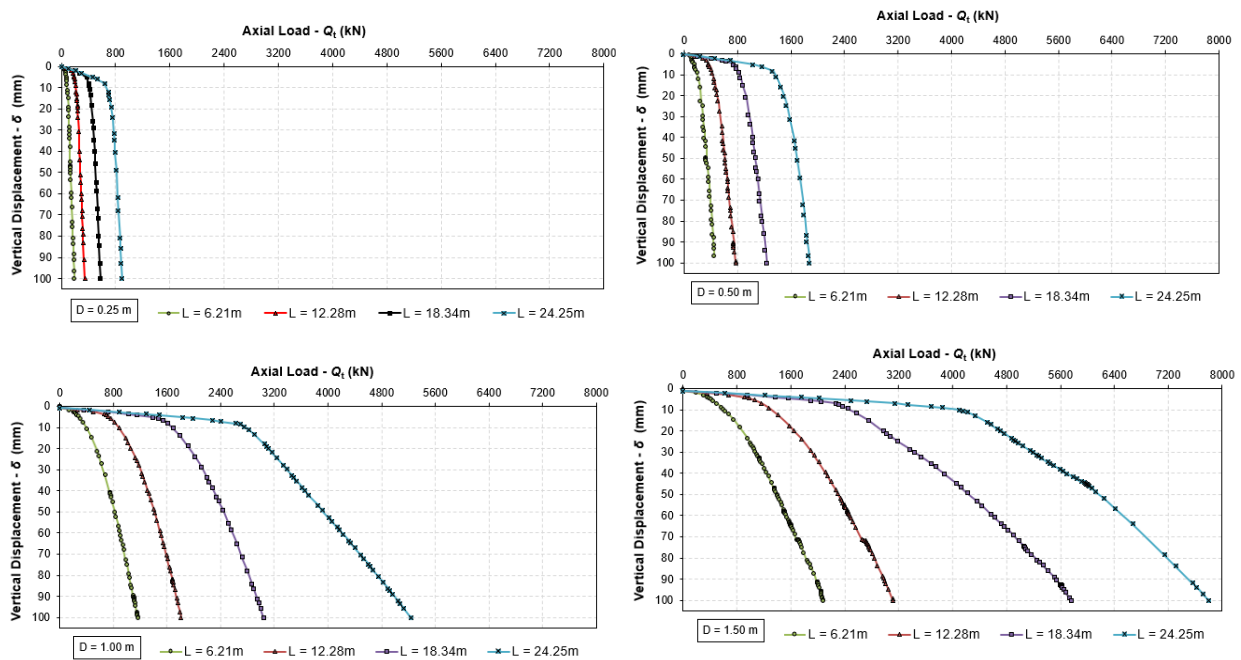


Figure 3. Load-displacement curves: a) $D = 0.25$ m, b) $D = 0.50$ m, c) $D = 1.00$ m, d) $D = 1.50$ m.

In Fig. 4, for a given pile displacement, both the total load (Q_t) and the total load per unit area (q_t) increase

non-linearly with the normalized length (L/D). The Q_t versus L/D curves for varying diameters display different behaviors, with steeper slopes as pile diameter increases. In contrast, the q_t versus L/D curves for different diameters exhibit a more consistent trend.

Normalizing the total load as $[(q_t/P_{atm}) \cdot (L/D)]$ results in the convergence of the four curves for each displacement (25 mm, 50 mm, 75 mm, and 100 mm) into a single curve, as depicted in Fig. 5a. This figure demonstrates that, for a given L/D , the normalized load $[(q_t/P_{atm}) \cdot (L/D)]$ is solely dependent on displacement. The atmospheric pressure (P_{atm}) is 101.325 kilopascals.

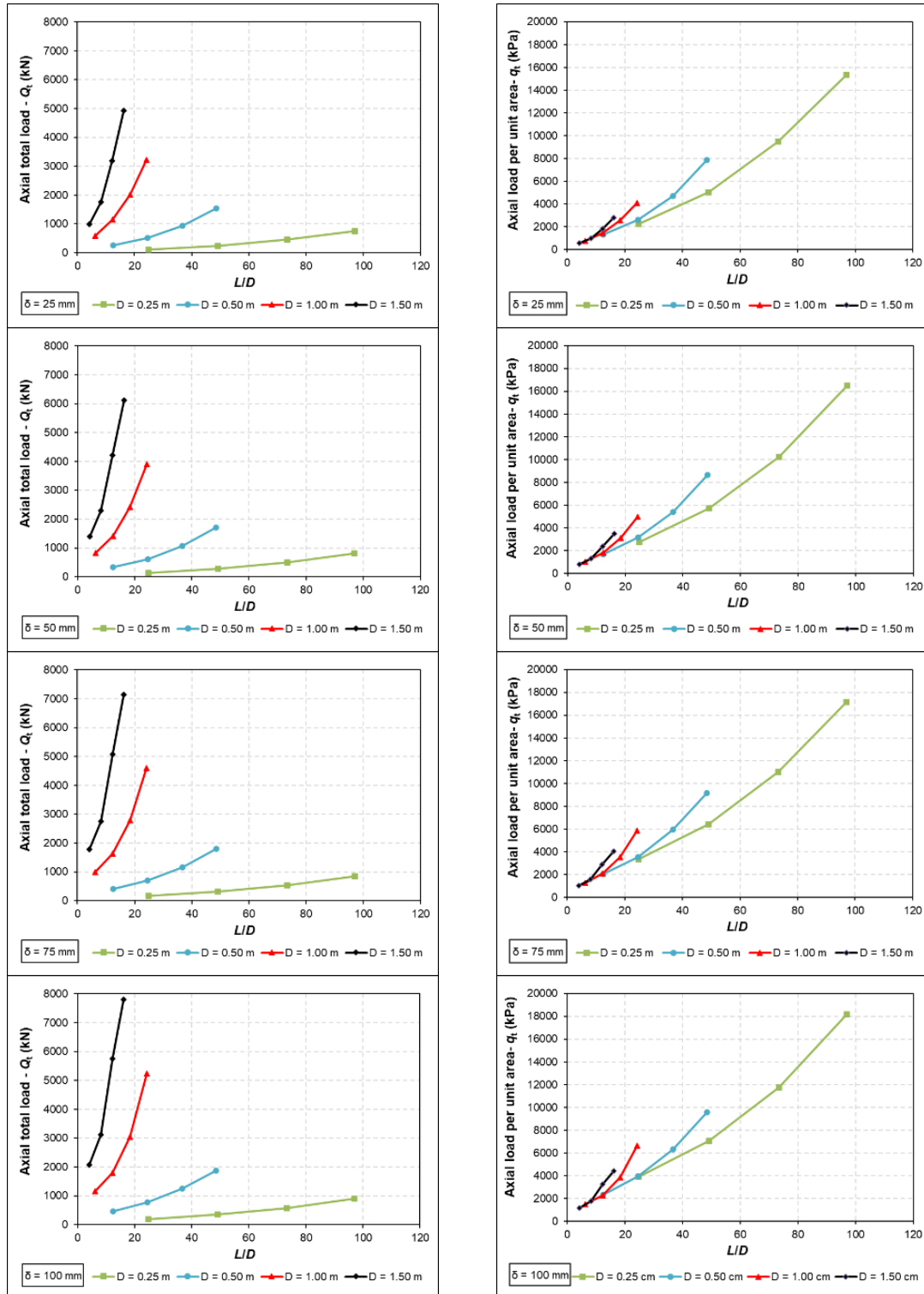


Figure 4. a) variation of total load and b) variation of total load per unit area versus L/D .

To eliminate the influence of displacement on the curves in Fig. 5a and obtain a single curve, the values of $[(q_t/P_{atm}) \cdot (L/D)]$ for each displacement were divided by their respective values corresponding to a displacement of 25 mm, as described by Eq. 2. Consequently, Fig. 5b illustrates the variation of the average λ_t as a function of the normalized displacement ($\delta/1''$), where 1 inch (1'') is equivalent to 25.4 mm. Equation 3 describes the relationship between λ_t and $\delta/1''$.

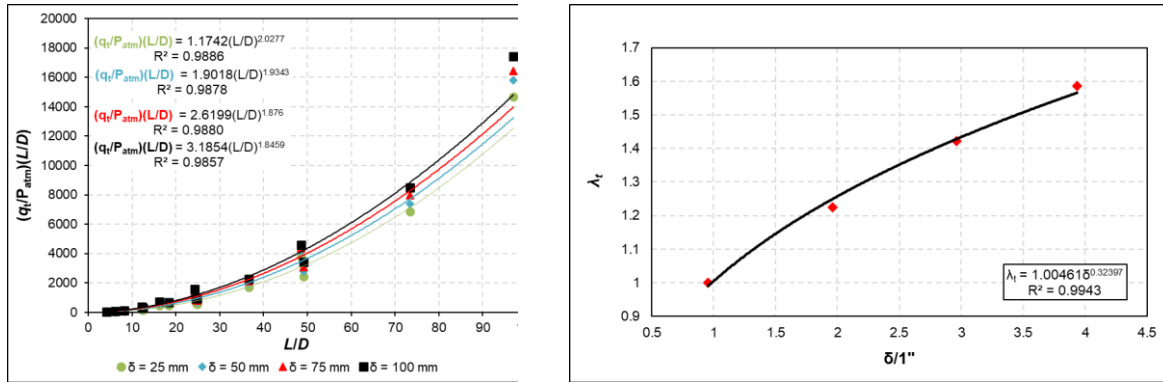


Figure 5. a) Normalized curves for each displacement, b) λ_t versus normalized displacement ($\delta/1''$).

$$\lambda_t = \frac{\left[\left(\frac{q_t}{P_{atm}}\right) \cdot \left(\frac{L}{D}\right)\right]_{\delta_i}}{\left[\left(\frac{q_t}{P_{atm}}\right) \cdot \left(\frac{L}{D}\right)\right]_{\delta=25\text{mm}}} \quad (2)$$

$$\lambda_t = 1.00461 \left(\frac{\delta}{1''}\right)^{0.32397} \quad (3)$$

The values of $[(q_t/P_{atm}) \cdot (L/D)]$ for each curve in Fig. 5a were divided by λ_t and then plotted as a function of L/D (Fig. 6a), thereby normalizing the 16 curves shown in Fig. 4. Equation 4 describes the curve shown in Fig. 7a and allows the prediction of the total load per unit area for a given displacement, considering different pile geometries. The generic expression for estimating load-displacement curve is given in Eq. 5, where the load factors N_{1t} , N_{2t} , and N_{3t} depend solely on the soil properties, and further studies with varying soil parameters are required to calibrate these factors. From a practical standpoint, a single load test curve obtained in homogeneous soil can be used to calibrate these factors. Once calibrated, the equation can then be applied to estimate the load-displacement curves for different piles installed at the same location. The subsequent validation of this equation using results from various load tests will not only promote the practical application of the method but also create opportunities for reducing both costs and time.

Figure 6b compares the normalized load values from Abaqus with those estimated by Eq. 4 to evaluate the accuracy of the proposed expression. The results show a high degree of agreement for low values of L/D , while a larger scatter is observed for higher values of L/D (slender piles).

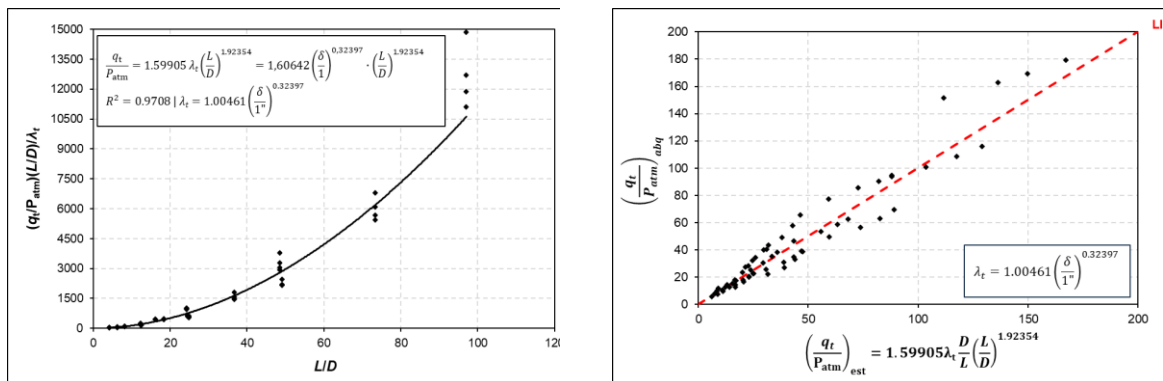


Figure 6. a) Normalized load versus L/D , b) comparison between Abaqus results and estimated results (Eq. 4).

$$\frac{q_t}{P_{atm}} = 1.59905 \lambda_t \cdot \left(\frac{L}{D}\right)^{1.92354} = 1.60642 \left(\frac{\delta}{1''}\right)^{0.32397} \cdot \left(\frac{L}{D}\right)^{1.92354} \quad (4)$$

$$\frac{q_t}{P_{atm}} = N_{1t} \cdot \left(\frac{\delta}{1''}\right)^{N_{2t}} \cdot \left(\frac{L}{D}\right)^{N_{3t}} \quad (5)$$

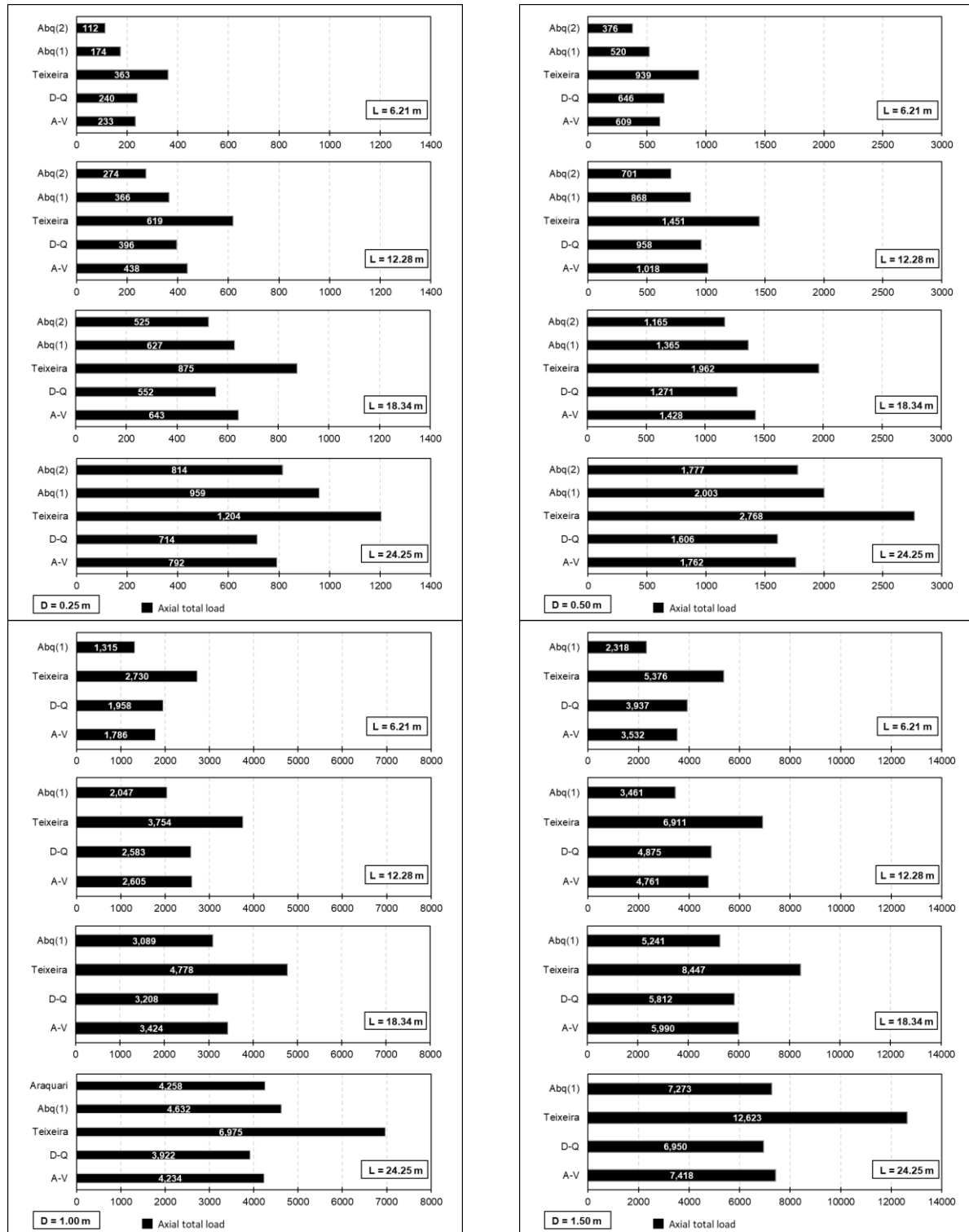


Figure 7. Comparison of total loads: numerical and semi-empiric results.

To assess the consistency of the simplifications made during the simulation, Figure 7 compares the results obtained from Abaqus with those estimated using semi-empirical methods. For clarity, Abq(1) considers Q_t values at a displacement of 100 mm, while Abq(2) considers Q_t values at displacements of 10% of the diameter. According to Salgado's [10], the ultimate load corresponding to a displacement of 10% of the pile diameter can be sufficient to induce operational failure or structural collapse of the element.

In general, the Teixeira (1996) method produced the highest Q_t values across all analyses, making it the least conservative method. The Q_t values from the other methods were in the same order of magnitude. For piles with diameters of 1.00 m or less, the Abaqus results showed lower Q_t values compared to the other methods and were closer to the results predicted by the Décourt-Quaresma and Aoki-Velloso methods. The small discrepancy may be due to methodological differences and simplifications resulting from layer homogenization. For larger pile lengths, regardless of diameter, the Décourt-Quaresma method gave more conservative results than the Aoki-Velloso method.

4 Conclusions

The paper proposes a normalized equation for predicting load-displacement curves based on the results of 16 numerical simulations involving different bored piles in homogeneous sandy soil.

A closer match between the experimental and numerical curves was observed, suggesting that the simplifications made can be considered reasonable for the purpose of this study. When comparing the loads obtained from numerical simulations and those estimated by semi-empirical methods, Teixeira's method proved to be the least conservative, estimating higher values for total load, tip resistance, and lateral friction. For longer piles, regardless of diameter, the Décourt-Quaresma produced more conservative total load estimates than the Aoki-Velloso. For piles with diameters less than or equal to 1.0 m, the Abaqus results showed lower total loads compared to other methods and were more consistent with the results of Décourt-Quaresma and Aoki-Velloso.

From a practical perspective, in homogeneous fields, the proposed equation can be a valuable tool for the preliminary estimation of load-displacement curves, provided that the load factors N_{1t} , N_{2t} , and N_{3t} - which depend solely on soil properties - are calibrated in advance. A single load test curve obtained in homogeneous soil can be used to calibrate these factors. Once calibrated, the equation can then be applied to estimate the load-displacement curves for different piles installed at the same location.

The approach presented in the paper is innovative; however, it may raise several questions due to the simplifications made in the numerical model. Consequently, ongoing research is focused on two main areas: 1) comparing the results of the proposed equation with those from experimental field tests, and 2) extending the equation to address non-homogeneous soils.

Authorship statement. The authors hereby confirm that they are the sole liable persons responsible for the authorship of this work, and that all material that has been herein included as part of the present paper is either the property (and authorship) of the authors, or has the permission of the owners to be included here.

References

- [1] W.G.K. Fleming. A new method for single pile settlement prediction and analysis. *Géotechnique*, v. 42, n. 3, p. 411–425, Sept. 1992.
- [2] J. Liu, H.B. Xiao, J. Tang, Q.S. Li. Analysis of load-transfer of single pile in layered soil. *Computers and Geotechnics*, v. 31, n. 2, p. 127-135, Jan. 2004.
- [3] N. Aoki, D.A. Velloso. An approximate method to estimate the bearing capacity of piles. *Proceedings, 5th. Pan American CSMFE, Buenos Aires, 1975*, vol.1, p. 367-376.
- [4] L. Décourt, A. R. Quaresma. Capacidade de carga de estacas a partir de valores de SPT. In: *COBRAMSEF*, 6., 1978, Rio de Janeiro. *Anais... Rio de Janeiro: ABMS, 1978*. v. 1, p. 45-54.
- [5] A. H. Teixeira. Projeto e Execução de Fundações. In: *Seminário de Engenharia de Fundações Especiais e Geotecnia*. São Paulo, 1996.
- [6] L. V. A. Lavallo. Estudo da interação solo-concreto das estacas escavadas do campo experimental de Araquari. *Dissertação (Mestrado em Engenharia Civil)*. Universidade Federal do Rio Grande do Sul, 2017.
- [7] F. A. Nienov. Desempenho de Estacas Escavadas de Grande Diâmetro em Solo Arenoso sob Carregamento Vertical. 2016. 267 p. Tese (Doutorado) - Programa de Pós-Graduação em Engenharia Civil, UFRGS – Porto Alegre, 2016.
- [8] G. F. Costa. Análise da Capacidade de Carga de Estacas Escavadas Submetidas ao Carregamento Vertical no Campo Experimental de Araquari: Métodos Semiempíricos e Modelagem Numérica. *Trabalho de Conclusão de Curso (Graduação em Engenharia Civil)*. Universidade Federal de Santa Catarina. Florianópolis, 2023.
- [9] N.C. Sampa, G.F. Costa, F.A. Nienov. Numerical analysis of large-diameter bored piles in sandy soil. In: *XLIV CILAMCE*, Portugal, nov. 2023.
- [10] R. Salgado. *The Engineering of Foundations*. McGraw-Hill, 2008